

---

This is an electronic reprint of the original article.  
This reprint may differ from the original in pagination and typographic detail.

Boev, O. V.; Puska, M. J.; Nieminen, R. M.  
**Electron and positron energy levels in solids**

*Published in:*  
Physical Review B

*DOI:*  
[10.1103/PhysRevB.36.7786](https://doi.org/10.1103/PhysRevB.36.7786)

Published: 15/11/1987

*Document Version*  
Publisher's PDF, also known as Version of record

*Please cite the original version:*  
Boev, O. V., Puska, M. J., & Nieminen, R. M. (1987). Electron and positron energy levels in solids. *Physical Review B*, 36(15), 7786-7794. <https://doi.org/10.1103/PhysRevB.36.7786>

---

This material is protected by copyright and other intellectual property rights, and duplication or sale of all or part of any of the repository collections is not permitted, except that material may be duplicated by you for your research use or educational purposes in electronic or print form. You must obtain permission for any other use. Electronic or print copies may not be offered, whether for sale or otherwise to anyone who is not an authorised user.

## Electron and positron energy levels in solids

O. V. Boev\* and M. J. Puska

*Laboratory of Physics, Helsinki University of Technology, SF-02150 Espoo, Finland*

R. M. Nieminen<sup>†</sup>

*Laboratory of Atomic and Solid State Physics, Cornell University, Ithaca, New York 14853-2501*

(Received 1 July 1987)

The self-consistent electron densities and the corresponding positron states are calculated for several metals and semiconductors in the local-density approximation of the density-functional formalism. The calculations are performed with the linear-muffin-tin-orbital band-structure method. The emphasis of this work is on the energy levels of the delocalized positron and the electron chemical potential which are now calculated with respect to the same potential reference. These energies determine quantities such as the positron and positronium work functions and the deformation potentials which are important parameters in slow-positron-beam experiments. The theoretical results are compared to values extracted from experiments.

### I. INTRODUCTION

The slow-positron-beam technique is a new powerful tool for studying solid surfaces and defect profiles as a function of the distance from the surface.<sup>1</sup> Positrons with a desired kinetic energy within a small energy spread are generated using a moderator crystal and subsequent acceleration in an electromagnetic field. In the sample, the first stage of the positron-solid interaction, slowing down and thermalization, results in a certain implantation profile. Thereafter positrons diffuse thermally in the solid and some of them are trapped by lattice defects. The essential point with respect to the slow-positron-beam experiments is that a large fraction of positrons can diffuse back to the surface and be emitted into the vacuum either as free positrons or (after picking up an electron from the surface) as positronium atoms. The trapping of positrons by the image potential at the surface is also possible.

The positron slowing-down process and the ensuing implantation profile can be well understood on the basis of the Monte Carlo simulations.<sup>2</sup> For the positron annihilation characteristics, i.e., the positron lifetime in delocalized or localized (trapped) states and for the momentum distribution of the annihilating positron-electron pair, there exist reliable and practical calculation methods,<sup>3-6</sup> which have proven their power in the interpretation of experimental findings. On the other hand, accurate calculations of positron trapping rates to crystal defects from the golden-rule formula are so far available for simple metals only.<sup>7</sup>

The purpose of this paper is to enlighten positron diffusion and surface emission. We calculate the positron band structure, in particular the bottom of the lowest-energy band, parallel with the self-consistent electron structure. The positron and electron energy levels in perfect bulk crystal directly give the positronium work function and, if the surface dipole potential is

known, also the positron work function. Moreover, the volume dependence of these levels (the deformation potential) can be used to estimate the positron-phonon coupling strength and thereby the positron diffusion constant.

The basis of the present calculations is the density-functional theory<sup>8</sup> in the local-density approximation (LDA) for exchange and correlation effects. It is first used in determining the self-consistent electron structures. The calculation of the delocalized positron Bloch states leans on the two-component generalization<sup>9</sup> of the density-functional theory. Also, in the case of positron states LDA is called for in the approximation of the electron-positron correlation. In practice, the electron and positron states are calculated by the linear-muffin-tin-orbital method (LMTO) within the atomic spheres approximation (ASA).<sup>10,11</sup> LMTO-ASA is one of the most efficient methods for electron-structure calculations. It has previously been used for positron states in bulk metals in order to determine the momentum distribution of the annihilating positron-electron pairs.<sup>12</sup> It has also been used for calculating positron states in bulk semiconductors and together with an associated Green's function technique for positron states trapped at monovacancies.<sup>13</sup> The main emphasis in the latter applications was the prediction of the positron lifetimes and binding energies at the vacancies. The positron lifetime depends on the volume integral of the product of the electron and positron densities and is therefore rather insensitive to small charge rearrangements in the system. Even a non-self-consistent electron density constructed by superimposing free-atom charge profiles can be sufficient for lifetime calculations.<sup>6</sup> On the contrary, the positron energy eigenvalue is very sensitive to the approximations made in calculating the electron structure. The sensitivity is reflected, e.g., in determining positron binding energies at defects. Therefore, the essential point in the present work is that electron densities used

as inputs for positron calculations are fully self-consistent.

## II. THEORY

In the density-functional theory the many-body problem of interacting electrons is cast in the form of a system of noninteracting particles sensing the effective potential

$$v_{\text{eff}}(\mathbf{r}) = \phi(\mathbf{r}) + v_{\text{xc}}(n(\mathbf{r})), \quad (1)$$

where  $\phi$  contains the Coulomb potential due to the external charges (nuclei) and the Hartree potential of the electron density  $n(\mathbf{r})$ . Equation (1) is written already in the LDA, in which  $v_{\text{xc}}$  is the exchange-correlation potential<sup>14</sup> depending at a given point  $\mathbf{r}$  on the electron density  $n(\mathbf{r})$  at that point only. The states of the noninteracting electrons are solved from the one-particle Schrödinger equation with the potential (1). Density-functional theory gives the *ground-state* electron density as the sum over the occupied states as

$$n(\mathbf{r}) = \sum_i |\psi(\mathbf{r})|^2. \quad (2)$$

The charge neutrality requires that these states are filled up to the Fermi level, which is given exactly as the corresponding energy eigenvalue solved from the one-particle Schrödinger equation.

The practical numerical solution of the above problem has been performed in this work using the LMTO-ASA method.<sup>10,11</sup> In ASA the crystal space is divided into spheres, the total volume of which is the total crystal volume. Potentials and charge densities are spherical averages within these spheres. In the case of cubic metals all spheres are centered around host nuclei and their radius is the Wigner-Seitz radius, while for semiconductors with diamond or zinc-blende structures half of the spheres are centered at interstitial sites. The use of the spherical densities and potentials near the nuclei is well justified. Neither is the geometry violation due to the ASA in the interstitial regions severe for the determination of the energy levels.<sup>15</sup>

The position of the Fermi level is given below with respect to the *crystal zero* level, which is defined as the Coulomb potential far away from a *single* atomic sphere. In the case of fcc and bcc metals all spheres are neutral in ASA and the Coulomb potential vanishes on the sphere surfaces fixing the potential reference. For the determination of the position of the Fermi level (or the crystal zero level) with respect to vacuum the potential due to the surface dipole is needed. This would require the calculation of the self-consistent electron structure for the surface. In this work, however, the surface dipole contributions are estimated using the experimental electron work functions and calculated bulk chemical potentials. This information is needed below for the calculation of the positron work function only. The different energy levels and the related quantities for electrons are shown schematically on the left-hand side of Fig. 1. The effective potential is fixed to the crystal zero. The self-consistent electron density calculation deter-

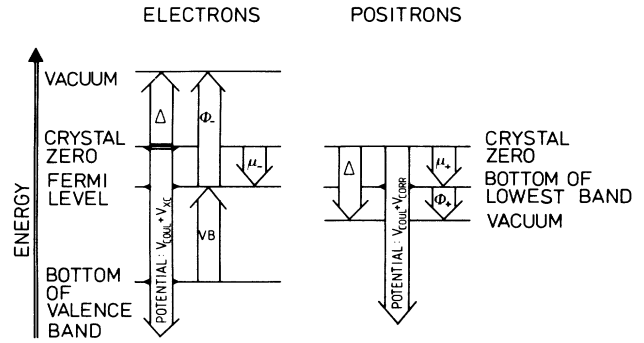


FIG. 1. Schematic view of electron and positron energy levels in a solid.  $\Delta$  is the dipole potential on the surface, VB the width of the valence band.  $\phi_-$  and  $\phi_+$  denote for the electron and positron work functions, respectively.  $\mu_-$  and  $\mu_+$  are the electron and positron chemical potentials, respectively.

mines the actual spatial form of the potential and fixes the energy levels, first of all the Fermi level, with respect to the reference potential. Figure 1 shows the surface dipole potential step ( $\Delta$ ) and the electron work function ( $\phi_-$ ) as the vacuum–crystal-zero and the vacuum–Fermi-level differences, respectively. These are positive quantities, as indicated by the arrows pointing upwards. The distance between the Fermi level and the crystal zero determines the electron chemical potential  $\mu_-$ . This is usually a negative quantity, as indicated by an arrow pointing downwards.

The complete many-body problem of interacting electrons and a positron can be treated in the two-component density-functional theory.<sup>9</sup> In the present work we are calculating the state of a positron delocalized over the whole crystal. For this situation of a low positron density the theory reduces to the following practical scheme. The self-consistent electron structure is first calculated without the positron as shortly described above. Thereafter, the potential sensed by the positron is constructed as

$$V^+(\mathbf{r}) = -\phi(\mathbf{r}) + V_{\text{corr}}(n(\mathbf{r})), \quad (3)$$

where  $\phi$  is the same Coulomb potential as in Eq. (1) and  $V_{\text{corr}}$  is the correlation potential, which describes the effects due to the short-range pileup of electrons near the positron.  $V_{\text{corr}}$  is treated in LDA as written in Eq. (3). For metals, the correlation potential  $V_{\text{corr}}^{\text{EG}}$  calculated<sup>16</sup> for a positron in a homogeneous electron gas is used, whereas in the case of semiconductors the potential is constructed as<sup>13</sup>

$$V_{\text{corr}}(n) = V_{\text{corr}}^{\text{EG}}(n)[f(n, \epsilon_g)]^{1/3}, \quad (4)$$

where

$$f(n, \epsilon_g) = 1 - \frac{0.37\epsilon_g}{1 + 0.18r_s}, \quad r_s = \left[ \frac{3}{4\pi n} \right]^{1/3}.$$

The same reduction factor  $f$  is used also in the calculation of positron annihilation rate. The rate calculations

allow us to fit the “gap” parameter  $\epsilon_g$  so that the experimental positron lifetime in a delocalized state is reproduced. It is found that the value of 0.2 for  $\epsilon_g$  describes well Si, Ge, and III-V compound semiconductors.<sup>13,17</sup> After the potential for the positron is constructed, the same methods (i.e., LMTO-ASA in this work) as for the electron can be used in solving the single-particle Schrödinger equation. The procedure for the positron states described is strictly valid (within LDA) only for the delocalized states. The problem of a positron localized due to a crystal defect and interacting with the surrounding electrons in principle requires the simultaneous self-consistent calculation of the electronic structure and the positron state.<sup>9</sup>

The important energy levels for a positron in a solid are shown schematically on the right-hand side of Fig. 1. The potential is fixed to the crystal zero and it is determined by the self-consistent electron density. It is essential to note that the crystal zero is common for electrons and positrons. The thermalized positrons are near the bottom of the lowest energy band at  $\mathbf{k}=0$ . The surface dipole potential for positrons is equal in magnitude as for electrons but opposite (negative) in sign. Therefore the vacuum level is below the crystal zero. Usually, the bottom of the lowest band is rather near the vacuum level. If the vacuum level is the lower one the positron work function  $\phi_+$  is negative as in Fig. 1. The positron chemical potential  $\mu_+$  is defined as the difference between the bottom of the lowest band and the crystal zero level and is usually negative.

If the solid is a heterostructure formed by different materials, the requirement that the Fermi level is the same everywhere in the solid determines the heights of the dipole steps at the interfaces. The differences in the positron affinities into different layers of the structure (“band offsets”) can thereafter be defined as the distances between “the bulk positron energy levels.” For the materials *A* and *B* in contact, the positron energy difference is thus

$$\Delta E_+^{A,B} = E_+^A - E_+^B = \mu_-^A - \mu_-^B + \mu_+^A - \mu_+^B. \quad (5)$$

This equation can be used also for predicting the affinity of positrons into precipitates in alloys (cf. the differences in positron pseudopotentials<sup>18</sup>).

The important quantities measured in slow-positron-beam experiments are closely related to the energy levels described above. The most directly related quantity is the maximum kinetic energy of positronium (Ps) atoms ejected into vacuum from the sample. The negative of this energy is called the positronium work function  $\phi_{Ps}$ . Actually, a more proper term would be positronium formation potential, since Ps is usually not stable *inside* close-packed solids. In the Ps ejection process an electron from the Fermi level and a positron from the bottom of the lowest energy band are taken out of the crystal into vacuum. This costs in energy the sum of the electron and positron work functions but when Ps is formed the binding energy of 6.8 eV is gained. Using the notation of Fig. 1 we write

$$\begin{aligned} \phi_{Ps} &= \phi_- + \phi_+ - 6.8 \text{ eV} \\ &= (-\mu_- + \Delta) + (-\mu_+ - \Delta) - 6.8 \text{ eV} \\ &= -\mu_- - \mu_+ - 6.8 \text{ eV}. \end{aligned} \quad (6)$$

Thus the Ps work function is a pure bulk property, independent of the surface dipole  $\Delta$ . Another fundamental quantity is the positron work function  $\phi_+$ . It depends on the surface dipole potential  $\Delta$  but we may eliminate  $\Delta$  by the help of the electron work function  $\phi_-$  as

$$\phi_+ = -\mu_+ - \Delta = -\mu_+ - \mu_- - \phi_-. \quad (7)$$

In this work we will use the experimental values for  $\phi_-$  in order to determine  $\phi_+$ .

The positron diffusion stage in a solid is dominated by the positron-phonon interactions. The coupling between a free particle and phonons is described in the deformation potential theory.<sup>19</sup> The strength of the coupling is determined by the deformation potential  $E_d^+$  which for a positron is the sum of the volume derivatives of positron and electron chemical potentials

$$E_d^+ = V \frac{\partial \mu_+}{\partial V} + V \frac{\partial \mu_-}{\partial V} = -V \frac{\partial \phi_{Ps}}{\partial V}. \quad (8)$$

Above, the inclusion of the electron part takes into account the maintaining of constant chemical potential in the presence of deformation. The volume derivatives of the chemical potentials are determined by performing self-consistent electron structure and positron calculations for a few slightly different lattice constants. The deformation potential theory gives the positron diffusion constant due to acoustic phonon scattering as

$$D = \left[ \frac{8\pi}{9} \right]^{1/2} \frac{\hbar^4 \langle c_{ii} \rangle}{(m^*)^{5/2} (k_B T)^{1/2} E_d^2}, \quad (9)$$

where  $m^*$  is the positron effective mass,  $T$  the absolute temperature, and  $\langle c_{ii} \rangle$  the elastic constant associated with longitudinal waves and averaged over the directions of propagation. The calculation of the average in  $\langle c_{ii} \rangle$  is a complicated numerical task and therefore we approximate it by

$$\langle c_{ii} \rangle \approx \frac{1}{2}(c_{11} + c_{12} + 2c_{44}). \quad (10)$$

This form is strictly valid for the (110) direction, but the variation corresponding to different directions is rather small, such that the uncertainty connected with Eq. (10) is much less than the uncertainty, e.g., due to  $m^*$  in calculating the diffusion constant. The effective positron mass  $m^*$  contains the contributions due to the periodic lattice (band effective mass  $m_b^*$ ) and due to the screening electron cloud (correlation effective mass  $m_{corr}^*$ ). The effective band mass is easy to determine by calculating the positron energy in few  $\mathbf{k}$  points near the bottom of the lowest energy band and by taking the curvature

$$m_b^* = \hbar^2 \left[ \frac{d^2 E}{dk^2} \right]^{-1}. \quad (11)$$

The determination of the correlation effective mass is a

difficult many-body problem<sup>20,21</sup> and the scatter between the results of different approximate solutions is considerable. The positron effective mass has been estimated from experiments in few cases. However, the quantitative interpretation of the experimental results is not unambiguous. Therefore we use throughout this work the value of  $m^*=1.5$  which is a compromise over the various theoretical and experimental determinations. This value is also consistent with the experimental order of magnitude for the diffusion constant, and we focus below more on the trends seen in the diffusion constants.

The temperature dependence of the electron and positron energy levels is related to the experimental determination of the deformation potential from the temperature dependence of the Ps work function.<sup>22,23</sup> The temperature influences  $\phi_{\text{Ps}}$  through (i) thermal expansion of the volume  $V$  of the solid and (ii) thermal vibrations of the atoms around their mean positions. From Eqs. (6) and (8) follows

$$\begin{aligned} \frac{d\phi_{\text{Ps}}}{dT} &= \frac{\partial V}{\partial T} \frac{\partial \phi_{\text{Ps}}}{\partial V} + \left[ \frac{\partial \phi_{\text{Ps}}}{\partial T} \right]_V \\ &= -\beta E_d^+ + \left[ \frac{\partial \phi_{\text{Ps}}}{\partial T} \right]_V, \end{aligned} \quad (12)$$

$$\begin{aligned} \left[ \frac{\partial \phi_{\text{Ps}}}{\partial T} \right]_V^{\text{vib}} &= - \left[ \frac{\partial \mu_-}{\partial T} \right]_V^{\text{vib}} - \left[ \frac{\partial \mu_+}{\partial T} \right]_V^{\text{vib}} \\ &\cong \left\langle -\frac{2m}{\hbar^2} \sum_{\mathbf{q} \neq 0} \frac{\partial |S(\mathbf{q})|^2}{\partial T} \frac{|w(\mathbf{q})|^2}{k_-^2 - |\mathbf{k}_+ + \mathbf{q}|^2} \right\rangle_{k_-} + \left\langle -\frac{2m}{\hbar^2} \sum_{\mathbf{q} \neq 0} \frac{\partial |S(\mathbf{q})|^2}{\partial T} \frac{|A(\mathbf{q})|^2}{k_+^2 - |\mathbf{k}_+ + \mathbf{q}|^2} (\mathbf{k}_+ \cdot \mathbf{q})^2 \right\rangle_{k_+}. \end{aligned} \quad (14)$$

Above, the summations in  $\mathbf{q}$  are over the Brillouin zone, and averages over  $k_- = k_F$  and  $k_+ \cong (3k_B T m^* / \hbar^2)^{1/2}$ , respectively.  $w(\mathbf{q})$  is the (local) electron pseudopotential, and

$$A(\mathbf{q}) = \frac{2}{\Omega} \int_{\Omega} d\mathbf{r} \frac{d}{dr} \ln[\psi_0(r)] j_1(qr) \quad (15)$$

is the positron "form factor"<sup>28</sup> [ $\psi_0(r)$  is the positron (pseudo) wave function and  $\Omega$  the unit cell volume]. The temperature dependence of the structure factor for a solid containing  $N$  unit cells can be approximated as

$$|S(\mathbf{q})|^2 \cong |S_0(\mathbf{q})|^2 + \left[ \frac{1}{N} - |S_0(\mathbf{q})|^2 \right] (1 - e^{-2W}), \quad (16)$$

where  $S_0(\mathbf{q})$  is the perfect lattice structure factor and  $W$  the Debye-Waller factor. When temperature rises, the  $\delta$  function peaks in  $S_0(\mathbf{q})$  at the reciprocal lattice vectors  $\mathbf{K}_n$  are scaled down, and simultaneously a diffuse background develops. For positrons, the net effect is the change in the summation weight in Eq. (14) to smaller  $q$  which makes  $\mu_+$  smaller:  $(\partial \mu_+ / \partial T)_V^{\text{vib}} < 0$ . Physically this means that thermal positrons can lower their energy

where  $\beta = (1/V)(\partial V / \partial T)$  is the thermal expansion coefficient. Thus a measurement of  $d\phi_{\text{Ps}}/dT$  can give the value of  $E_d$ , provided that the temperature derivative  $(\partial \phi_{\text{Ps}} / \partial T)_V$  is known. Unfortunately, a precise determination of the constant volume derivative is difficult, as exemplified by the large scatter in the estimates for the corresponding quantity for the electron work function.<sup>24-26</sup>

From Eq. (6), we have

$$\left[ \frac{\partial \phi_{\text{Ps}}}{\partial T} \right]_V = - \left[ \frac{\partial \mu_-}{\partial T} \right]_V - \left[ \frac{\partial \mu_+}{\partial T} \right]_V. \quad (13)$$

The purely electronic contribution to  $(\partial \mu_- / \partial T)_V$  is proportional to  $(k_B T / \epsilon_F) k_B$  and thus exceedingly small. One is left with the effect of harmonic lattice vibrations  $(\partial \mu_- / \partial T)_V^{\text{vib}}$  and  $(\partial \mu_+ / \partial T)_V^{\text{vib}}$ . Let us examine these in terms of perturbation theory based on weak electronic<sup>27</sup> and positron pseudopotentials.<sup>18,28</sup> Since harmonic vibrations do not change the average value of the electron (positron)-ion interaction, the temperature derivatives arise from the second-order term, which involves the structure factor  $S(\mathbf{q}; T)$ . One finds

by adjusting to instantaneous ionic density fluctuations. Because of the larger energy denominators ( $k_F \gg k_+$ ), diffuse scattering does not affect electrons as much, and the Debye-Waller damping acts to change the sign of  $(\partial \mu_- / \partial T)_V^{\text{vib}}$  from negative to positive.

Accurate numerical estimates are difficult to obtain.<sup>24-26</sup> The point is that while some cancellation between  $(\partial \mu_- / \partial T)_V^{\text{vib}}$  and  $(\partial \mu_+ / \partial T)_V^{\text{vib}}$  is likely, there is *no a priori reason* to assume the second term in Eq. (12) to vanish identically, as was done by Gullikson and Mills<sup>22</sup> when they determined  $E_d$  from the temperature variation of  $\phi_{\text{Ps}}$ . However, if one makes the assumption that  $(\partial \phi_{\text{Ps}} / \partial T)_V = c$ , a (temperature independent) constant, the data of Gullikson and Mills seem to be consistent with a very small value for  $c$ . At low  $T \ll \Theta_{\text{Debye}}$  for metals,  $\beta(T) = \gamma T$ , while at higher  $T$ ,  $\beta \approx \text{const}$ . Thus the zero-temperature slope of  $\phi_{\text{Ps}}$  versus  $T$  should give  $\beta$ . It is close to zero for the Al data of Gullikson and Mills.

### III. RESULTS AND DISCUSSION

We have calculated by the LMTO-ASA method the self-consistent electronic structure for several simple and transition metals as well as for the semiconductors Si

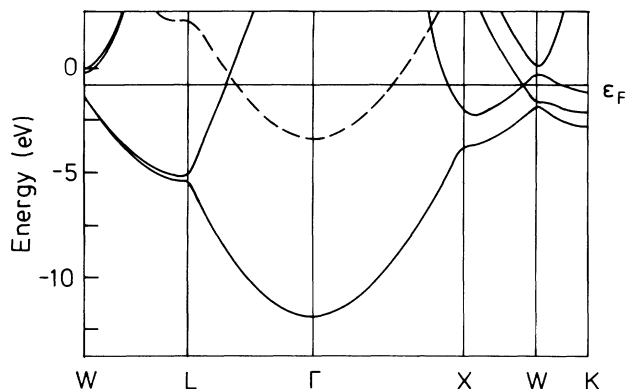


FIG. 2. The electron (solid lines) and positron (dashed lines) band structures for Al.

and Ge. The lattice constants corresponding to room temperature have been used. The calculated electron band structure and the lowest positron band in Al are shown in Fig. 2. The positron band is rather free-particle-like and resembles closely the lowest valence electron band. Also, the positron effective band mass at the  $\Gamma$  point is near the free-particle mass,  $m_b^* = 1.01$  (for other metals we find larger band masses, but  $m_b^* < 1.10$  in all cases studied). The lattice structures and lattice constants used and the calculated chemical potentials for electrons and positrons are collected in Table I. The electron chemical potential, i.e., the position of the Fermi level, depends on the details of the electron band structure. For transition metals the values of electron chemical potential and its volume derivative presented in Table I are in agreement with the results of Andersen *et al.*<sup>10</sup> The positron chemical potential can be divided into a correlation ( $E_{\text{corr}}$ ) and zero-point parts ( $E_0$ ) (Refs. 3 and 29)

$$\mu_+ = E_0 + E_{\text{corr}}, \quad (17)$$

with

$$E_0 = \frac{\hbar^2}{2m} \int dr \psi_+(\mathbf{r}) \left[ -\frac{1}{2} \nabla^2 - \phi(\mathbf{r}) \right] \psi_+(\mathbf{r}), \quad (18)$$

and

$$E_{\text{corr}} = \int d\mathbf{r} |\psi_+(\mathbf{r})|^2 V_{\text{corr}}(n(r)), \quad (19)$$

where  $\psi_+$  is the positron wave function. The negative correlation energy dominates over the positive zero-point energy. This dominance is stronger the more open the lattice structure is. In the volume derivative  $V(\partial\mu_+/\partial V)$  the negative zero-point contribution is usually larger in magnitude than the positive correlation contribution, but in the case of open semiconductor lattices the latter dominates and the derivative is positive.

From the calculated chemical potentials the positronium work function  $\phi_{\text{Ps}}$  can be directly deduced via Eq. (6). The values obtained are shown in Table II and compared with the available experimental data from positronium time-of-flight measurements.<sup>30</sup> The experimental trend is reproduced and also the quantitative agreement is satisfactory when the large experimental error bars are taken into account. It is interesting to note that the theory predicts a slightly positive positronium work function for Si. This theoretical value is calculated with the electron chemical potential coinciding with the top of the valence band. If the chemical potential is higher in the band gap, the positronium work function becomes negative. Thus Ps emission from Si should be sensitive to doping. Also in Table II, the theoretical positron work functions, calculated by the help of the experimental electron work functions via Eq. (7), are compared with the experimental ones measured directly in the slow-positron-beam experiments.<sup>31,32</sup> In most cases the experimental trends are found and the absolute values are reproduced within few tenths of eV. Si seems to be an exception: theory predicts that the positron work

TABLE I. Calculated chemical potentials and their volume derivatives for electrons [ $\mu_-$  and  $V(\partial\mu_-/\partial V)$ ] and positrons [ $\mu_+$  and  $V(\partial\mu_+/\partial V)$ ]. The lattice structures and constants ( $a$ ) used are also given. They correspond to the room temperature, with the exception of the 5-K value for potassium, for which the melting point is 20 K.

Host	Lattice structure	$a$ (units of $a_0$ )	$\mu_-$ (eV)	$\mu_+$ (eV)	$V \frac{\partial\mu_-}{\partial V}$ (eV)	$V \frac{\partial\mu_+}{\partial V}$ (eV)
Na	bcc	7.987	-2.32	-4.80	-1.61	-0.98
K	bcc	9.877	-2.25	-4.80	-1.77	-1.41
Al	fcc	7.656	-0.74	-3.35	-6.00	-1.70
Cr	bcc	5.463	-0.42	-4.57	-9.33	-2.50
Ni	fcc	6.654	-1.55	-2.91	-8.13	-2.36
Cu	fcc	6.824	-1.59	-3.22	-7.39	-2.06
Ag	fcc	7.732	-2.14	-3.22	-7.23	-2.25
Mo	bcc	5.955	-0.04	-1.88	-11.25	-3.06
Pb	fcc	9.357	-1.58	-3.98	-4.81	-1.58
Si	dia	10.261	-0.54	-6.41	-7.51	+1.32
Ge	dia	10.696	-0.60	-6.19	-7.64	+1.02

function is clearly positive whereas the experimental value is  $-1.0$  eV. Si may be a difficult case for slow-positron-beam experiments due to the charging of the surfaces causing an extra electric field, and impurities on the surface may also hinder the accurate determination of the work functions. However, the rather successful comparison between the experimental and theoretical results gives credence to the theoretical models used, especially to the LDA for electron-exchange correlation and positron-electron correlation. Previously,<sup>3,29,33,34</sup> the positron and positronium work functions have been calculated in a more indirect way than in the present work, which is the first to accurately solve the electron and positron states in a crystalline potential. Another difference is that in the previous calculations the Schrödinger equation for positron is solved with only the Coulomb part of the total potential (3) for the “zero-point” energy  $E_0$ , and the correlation energy  $E_{\text{corr}}$  is determined using electron gas results with an average host electron density. The old treatment can be justified by the fact that the positron wave function is concentrated in the interstitial regions, where the positron sees an approximately uniform valence electron density. While the trends in the work functions are usually the same in all calculations, there exist differences of up to 1 eV in the absolute values between the present and earlier cal-

culations. These kind of disagreements exist also between the different calculations employing the old schemes indicating perhaps the importance of the self-consistent determination of the electron structure. The present direct LDA scheme treats the simple and transition metals as well as the semiconductors on the same more fundamental footing provided by the density-functional theory.

The chemical potentials listed in Table I can be directly used in estimating the positron affinity to different materials in heterostructures. For example, for Cu and Ag in contact, positron favors Ag with the affinity difference of  $\Delta E_+^{\text{Cu,Ag}} = 0.55$  eV. This affinity difference results purely from the dipole step on the Cu-Ag interface, because the chemical potentials for positrons are equal in these metals. The lower chemical potential for electrons in Ag than in Cu reflects the smaller  $d$ -band width of Ag. Experimentally, the affinity difference between Cu and Ag manifests itself as a “positron-diode effect”<sup>35</sup> in the slow-positron-beam measurements. Namely, if a few layers of Cu are evaporated on Ag the positronium emission out of the sample is strongly reduced in comparison to the case when the sample is prepared by evaporating Ag on Cu.<sup>36</sup> In the former case thermalized positrons are held far from the surface by the potential barrier due to the Cu coverage.

TABLE II. Comparison of the theoretical positronium and positron work functions with the experimental ones. The theoretical values are calculated from Eqs. (6) and (7) using the data in Table I and the experimental electron work functions listed below.

Host	$\phi_{\text{Ps}}^{\text{theor}}$ (eV)	$\phi_{\text{Ps}}^{\text{expt a}}$ (eV)	Surface	$\phi_{-}^{\text{expt b}}$ (eV)	$\phi_{+}^{\text{theor}}$ (eV)	$\phi_{+}^{\text{expt c}}$ (eV)
Al	-2.71	$-2.78 \pm 0.28$	(100)	4.41	-0.32	-0.19
			(110)	4.28	-0.19	-0.05
			(111)	4.24	-0.15	-0.04
Cr	-4.10		(100)	4.46	-1.76	-1.76
Ni	-2.35	$-2.63 \pm 0.26$	(100)	5.22	-0.77	-1.11
			(110)	5.04	-0.59	
			(111)	5.35	-0.90	
Cu	-1.99	$-2.50 \pm 0.25$	(100)	4.59	+0.22	> 0
			(110)	4.48	+0.33	-0.13
			(111)	4.94	-0.13	-0.40
Ag	-1.44		(100)	4.64	+0.72	> 0
			(110)	4.52	+0.84	
			(111)	4.74	+0.62	> 0
Mo	-4.88		(100)	4.53	-2.65	
			(110)	4.95	-3.03	
			(111)	4.55	-2.67	< -3
Pb	-1.25	$-0.73 \pm 0.07$	(100)	4.01	+1.55	> 0
Si	+0.15		(100)	4.91	+2.04	
			(111)	4.74	+2.21	-1.0
Ge	-0.02		(111)	4.8	+1.98	> 0

<sup>a</sup>Reference 30.

<sup>b</sup>References 25 and 31.

<sup>c</sup>References 31 and 32.

TABLE III. Positron diffusion constants at 300 K.  $E_d^{+, \text{theor}}$  is the deformation potential calculated from Eq. (8) using the volume derivatives of the chemical potentials listed in Table I. The experimental values of  $E_d^{+, \text{expt}}$  are based on the values of  $d\phi_{\text{ps}}/dT$  at  $T=300$  K, and the corresponding values of thermal expansion coefficient (Ref. 39). The average elastic constant  $\langle c_{ii} \rangle$  is calculated from Eq. (10) using experimental elastic data (Ref. 38). For the effective positron mass  $m^*$  the value of 1.5 is used for all hosts. The diffusion constant  $D$  is determined then via Eq. (9).

Host	$E_d^{+, \text{theor}}$ (eV)	$E_d^{+, \text{expt}}$ (eV)	$\langle c_{ii} \rangle$ ( $10^{12}$ dyn cm $^{-2}$ )	$D^{\text{theor}}$ (cm $^2$ s $^{-1}$ )	$D^{\text{expt}}$ (cm $^2$ s $^{-1}$ )
Na	-2.59		0.144	1.29	
Al	-7.70	-10.8, <sup>a</sup> -13.4 <sup>b</sup>	1.12	1.13	0.76 <sup>c</sup>
Cr	-11.83		3.10	1.27	
Ni	-10.49	-9.0, <sup>c</sup> -13.9 <sup>b</sup>	3.25	1.77	
Cu	-9.45	-10.1, <sup>c</sup> -14.6 <sup>b</sup>	2.21	1.49	1.06 <sup>f</sup>
Ag	-9.48		1.53	1.02	
Mo	-14.31		4.21	1.24	1.2 <sup>g</sup>
Pb	-6.39	-6.11 <sup>d</sup>	0.61	0.86	
Si	-6.19		1.94	3.05	2.7, <sup>h</sup> 1.56 <sup>f</sup>
Ge	-6.62		1.55	2.13	0.5, <sup>i</sup> 0.55 <sup>f</sup>

<sup>a</sup>Reference 22.

<sup>b</sup>Reference 23.

<sup>c</sup>Reference 40.

<sup>d</sup>Reference 41.

<sup>e</sup>Reference 30.

<sup>f</sup>Reference 31.

<sup>g</sup>Reference 32.

<sup>h</sup>Reference 42.

<sup>i</sup>Reference 43.

The calculated positron deformation potentials and diffusion constants are collected in Table III. The deformation potentials for simple metals agree within 1 eV with the previous estimates by Bergersen *et al.*<sup>37</sup> who estimated the deformation potential from derivatives of positron and electron chemical potentials, the positron contribution consisting of the zero-point and correlation energy parts. The three terms were estimated separately using different kinds of arguments. In contrast with that, the present results are based on systematic LDA calculations. Moreover, the present calculations are straightforwardly extended beyond this simple metals to include transition metals and semiconductors.

In order to make more contact with the old results by Bergersen *et al.*<sup>37</sup> we have calculated the zero-point and correlation energy contributions for Al using Eqs. (18) and (19). The comparison of the results is made in Table IV. We show also the positron values which we have obtained by a calculation method<sup>6</sup> based on the superposition of free atoms and the numerical solution of the full three-dimensional (3D) Schrödinger equation. Both of the present calculations use the same LDA for electron-positron correlation energy and consistently the correlation contributions calculated via the simple integrals of Eq. (19) are very close to each other. The potential calculated from the self-consistent LMTO-ASA electron density is steeper than that calculated from the superimposed atomic charges because of the electron charge transfer towards to the interstitial regions in the former case relative to the latter one. This tendency is reflected as a larger zero-point energy in the LMTO-ASA calculations than in 3D; the values of  $E_0$  are 4.99 eV and 4.23 eV, respectively. The volume dependence of  $E_0$  is for the same reason stronger in the former method as can be seen in Table IV. In the work by Bergersen

*et al.*<sup>37</sup> the volume derivatives  $V(\partial E_{\text{corr}}/\partial V)$  and  $V(\partial \mu_-/\partial V)$  are estimated in the uniform electron gas model and therefore they deviate somewhat from the present values. However, the overall agreement is surprisingly good. Moreover, it is interesting to note that the simple RPA estimate,  $E_d = -2\epsilon_F/3$  ( $\epsilon_F$  is the valence electron gas Fermi energy), gives  $E_d = -7.79$  eV.

Experimentally, the positron deformation potential in Al has been determined from the temperature dependence of the positronium work function by Gullikson and Mills.<sup>22</sup> Their value of -11.6 eV is remarkably larger in magnitude than our result -7.70 eV. While the reason for this discrepancy is not clear, the omission of the term  $(\partial \phi_{\text{ps}}/\partial T)_V$  in Eq. (12) may affect the experimental value as discussed above. Table III also includes other experimental estimates for  $E_d$  based on the slope of  $\phi_{\text{ps}}$  versus  $T$  at 300 K, and the values of the thermal expansion coefficient<sup>39</sup> at that temperature, i.e., assuming

TABLE IV. The various contributions to the positron deformation potential in Al. In the present calculations (LMTO-ASA and 3D) the zero-point [ $V(dE_0/dV)$ ] and the correlation [ $V(dE_{\text{corr}}/dV)$ ] parts are calculated using Eqs. (18) and (19).

	$V \frac{dE_0}{dV}$ (eV)	$V \frac{dE_{\text{corr}}}{dV}$ (eV)	$V \frac{d\mu_-}{dV}$ (eV)	$E_d^+$ (eV)
LMTO-ASA	-3.42	+1.72	-6.00	-7.70
3D	-2.76	+1.74		
Bergersen <i>et al.</i> <sup>a</sup>	-2.2	+1.4	-7.8	-8.6

<sup>a</sup>Reference 37.



$(\partial\phi_{\text{Ps}}/\partial T)_V$  to be zero. The scatter in these numbers is rather large, as the slope is difficult to determine accurately. However, the calculated values seem to lie below the experimental ones pointing again to the possible role of  $(\partial\phi_{\text{Ps}}/\partial T)_V$ .

The positron diffusion constants are calculated using the deformation potential model via Eq. (9) and shown in Table III. The value of 1.5 was used for the positron effective mass  $m^*$  for all hosts. This value is in accord with the recent experimental determination<sup>21</sup> of the effective mass in potassium and reproduces well the overall order of magnitude of the diffusion constants. The main importance of the theoretical results for diffusion constant shown in Table III is in the trends between different hosts. The magnitudes are certainly affected by the dependence of the effective mass on the host, especially when the lattice and band structures differ considerably. However, we are tempted to believe the overall trends. Unfortunately, the experimental results collected in Table III are obtained by several different methods and are therefore not directly comparable. The larger value for Ge and the smaller value for Si are from mobility measurements<sup>31</sup> in which a bias electric field is applied across a semiconductor detector. The other values are obtained by analyzing the slow positron data for the Ps fraction as a function of the incident positron energy. Unfortunately, except in the case of Mo, the slow positron results shown in Table III may be affected by the incorrect analysis in which the effects due to epithermal positrons was not suppressed. Their contribution may even affect the apparent temperature dependence<sup>44</sup> of the positron diffusion constant, which is  $T^{-1/2}$  according to the deformation potential model. This dependence was accurately reproduced in the recent analysis<sup>32</sup> of experimental data for Mo. This analysis gave for the diffusion constant at 300 K the

value of  $1.2 \text{ cm}^2 \text{ s}^{-1}$  given in Table III. This is the most reliable published value thus far, and in excellent agreement with the value calculated here. However, given the uncertainty in the effective mass, we may conclude from Table III that theory and different experiments are in a qualitative agreement (with the possible exception of Ge).

#### IV. CONCLUSIONS

We have performed up to date band-structure calculations for electron and positron energetics in solids. The principle is simple: First the electron structure, i.e., electron density, energy levels, and the effective potential, is solved self-consistently within LDA for electron exchange and correlation. Thereafter the potential for positrons is known in LDA for electron-positron correlation and the positron energy bands can be calculated. The values for positron and positronium work functions obtained are compared with the available experimental data and the good agreement gives credence to the LDA's used. The chemical potentials for positrons and electrons are now calculated for several solids on the same footing and therefore they are valuable in determining the positron affinity to different materials or phases in heterostructures or in precipitate systems. Moreover, the volume dependences of the chemical potentials determine the positron deformation potential which can be used to describe the positron-phonon interaction and the ensuing phonon limited positron diffusion. In conclusion, the scheme presented, being able to predict quantities directly measurable by slow-positron-beam techniques, is a useful tool to be employed as a support to the experiments concerning various kinds of problems of bulk solids and solid surfaces.

\*Permanent address: Tomsk Polytechnical Institute, Tomsk, 634004, USSR.

<sup>†</sup>Permanent address: Laboratory of Physics, Helsinki University of Technology, SF-02150 Espoo, Finland.

<sup>1</sup>*Positron Solid State Physics*, edited by W. Brandt and A. Dupasquier (North-Holland, Amsterdam, 1983).

<sup>2</sup>S. Valkealahti and R. M. Nieminen, *Appl. Phys. A* **32**, 95 (1983); *ibid.* **35**, 51 (1984).

<sup>3</sup>C. H. Hodges and M. J. Stott, *Phys. Rev. B* **7**, 73 (1973).

<sup>4</sup>M. Manninen, R. M. Nieminen, P. Hautojärvi, and J. Arponen, *Phys. Rev. B* **12**, 4012 (1975).

<sup>5</sup>R. P. Gupta and R. W. Siegel, *Phys. Rev. Lett.* **39**, 1212 (1977).

<sup>6</sup>M. J. Puska and R. M. Nieminen, *J. Phys. F* **13**, 333 (1983).

<sup>7</sup>M. J. Puska and M. Manninen, *J. Phys. F* (to be published).

<sup>8</sup>*Theory of the Inhomogeneous Electron Gas*, edited by S. Lundqvist and N. H. March (Plenum, New York, 1983).

<sup>9</sup>E. Boroński and R. M. Nieminen, *Phys. Rev. B* **34**, 3820 (1986).

<sup>10</sup>O. K. Andersen, O. Jepsen, and D. Glötzel, in *Highlights of Condensed-Matter Theory*, edited by F. Bassani, F. Fumi, and M. P. Tosi (North-Holland, Amsterdam, 1985).

<sup>11</sup>H. C. Skriver, *The LMTO Method* (Springer, New York, 1984).

<sup>12</sup>A. K. Singh and T. Jarlborg, *J. Phys. F* **15**, 727 (1985).

<sup>13</sup>M. J. Puska, O. Jepsen, O. Gunnarsson, and R. M. Nieminen, *Phys. Rev. B* **34**, 2695 (1986).

<sup>14</sup>D. M. Ceperley and B. J. Alder, *Phys. Rev. Lett.* **45**, 566 (1980); we use their local exchange-correlation functional as parametrized by J. Perdew and A. Zunger, *Phys. Rev. B* **23**, 5048 (1981).

<sup>15</sup>D. Glötzel, B. Segall, and O. K. Andersen, *Solid State Commun.* **36**, 403 (1980).

<sup>16</sup>J. Arponen and E. Pajanne, *Ann. Phys. (N.Y.)* **121**, 343 (1979); *J. Phys. F* **9**, 2359 (1979); we use their data for the electron-positron correlation potential as parametrized in Ref. 9.

<sup>17</sup>M. J. Puska (unpublished).

<sup>18</sup>M. J. Stott and P. Kubica, *Phys. Rev. B* **11**, 1 (1975).

<sup>19</sup>J. Bardeen and W. Shockley, *Phys. Rev.* **80**, 72 (1950).

<sup>20</sup>H.-J. Mikeska, *Z. Phys.* **232**, 159 (1970); M. Baldo and R. Pucci, *Nuovo Cimento* **23B**, 202 (1974); A. Isii, *Phys. Lett.* **88A**, 417 (1982).

<sup>21</sup>T. Hyodo, T. McMullen, and A. T. Stewart, *Phys. Rev. B* **33**,

- 3050 (1986).
- <sup>22</sup>E. M. Gullikson and A. P. Mills, *Phys. Rev. B* **35**, 8759 (1987).
- <sup>23</sup>I. J. Rosenberg, R. H. Howell, and M. J. Fluss, *Phys. Rev. B* **35**, 2083 (1987).
- <sup>24</sup>C. Herring and M. H. Nichols, *Rev. Mod. Phys.* **21**, 185 (1949).
- <sup>25</sup>J. Hölzl and F. K. Schulte, in *Solid Surface Physics*, Vol. 85 of *Springer Tracts in Modern Physics* (Springer, Berlin, 1979).
- <sup>26</sup>A. Kiejna, *Surf. Sci.* **178**, 349 (1986).
- <sup>27</sup>W. A. Harrison, *Pseudopotentials in the Theory of Metals* (Benjamin, New York, 1966).
- <sup>28</sup>P. Kubica and M. J. Stott, *J. Phys. F* **4**, 1969 (1974).
- <sup>29</sup>R. M. Nieminen and C. H. Hodges, *Solid State Commun.* **18**, 1115 (1976).
- <sup>30</sup>R. H. Howell, I. J. Rosenberg, M. J. Fluss, R. E. Goldberg, and R. B. Laughlin, *Phys. Rev. B* **35**, 5303 (1987); R. H. Howell, I. J. Rosenberg, P. Meyer, and M. J. Fluss, *ibid.* **35**, 4555 (1987).
- <sup>31</sup>A. P. Mills, *Positron Solid State Physics*, Ref. 1, p. 432.
- <sup>32</sup>H. Huomo, A. Vehanen, M. D. Bentzon, and P. Hautojärvi, *Phys. Rev. B* **35**, 8252 (1987).
- <sup>33</sup>R. M. Nieminen and J. Oliva, *Phys. Rev. B* **22**, 2226 (1980).
- <sup>34</sup>G. Fletcher, J. L. Fry, and P. C. Pattnaik, *Phys. Rev. B* **27**, 3987 (1983).
- <sup>35</sup>M. Debowska, R. Evertowski, and W. Swiatkowski, *Appl. Phys. A* **36**, 47 (1985).
- <sup>36</sup>P. Huttunen, A. Vehanen, and P. Hautojärvi (unpublished).
- <sup>37</sup>B. Bergersen, E. Pajanne, P. Kubica, M. J. Stott, and C. H. Hodges, *Solid State Commun.* **15**, 1377 (1974).
- <sup>38</sup>G. Leibfried and N. Breuer, *Point Defects in Metals I*, Vol. 81 of *Springer Tracts in Modern Physics* (Springer, Berlin, 1978).
- <sup>39</sup>Y. S. Touloukian, R. K. Kirby, R. E. Taylor, and P. D. Desai, *Thermal Expansion of Metallic Elements and Alloys*, Vol. 12 of *Thermophysical Properties of Matter* (IFI/Plenum, New York-Washington, 1975).
- <sup>40</sup>D. A. Fischer, K. G. Lynn, and D. W. Gidley, *Phys. Rev. B* **33**, 4479 (1986).
- <sup>41</sup>P. J. Schultz and K. G. Lynn, *Phys. Rev. B* **26**, 2390 (1982).
- <sup>42</sup>B. Nielsen, K. G. Lynn, and A. Vehanen, *Phys. Rev. B* **32**, 2296 (1985).
- <sup>43</sup>H. H. Jorch, K. G. Lynn, and I. K. Mackenzie, *Phys. Rev. Lett.* **47**, 362 (1981); H. H. Jorch, K. G. Lynn, and T. McMullen, *Phys. Rev. B* **30**, 93 (1984).
- <sup>44</sup>P. J. Schultz, K. G. Lynn, and B. Nielsen, *Phys. Rev. B* **32**, 1369 (1985).